China Steel Technical Report, No. 31, pp.52－59, (2018)

Microstructural Simulation of a 5052 Aluminum Alloy Strip for a Hot Tandem Mill

SHI-RONG CHEN and YI-FAN KAO

New Materials Research & Development Department
China Steel Corporation

Evolution of microstructure in a 5052 hot-rolled strip has been investigated using the hot plane strain compression test with a Gleeble 3800 simulator. Single and two pass compressions were carried out respectively during which fast cooling at the end of the compression was applied. As-compressed samples were annealed by the cooling pattern of mill coiling to simulate the hot-rolled strips. The annealing effect was analyzed by Arrhenius law and Avrami equation. Effects of rolling parameters on recrystallization behaviors was quantitatively assessed by isothermal annealing. It was found that an as-deformed structure recrystallizes during the subsequent annealing and the recrystallization is promoted by decreasing rolling temperature, interpass time, or by increasing strain rate, accumulated strain as well as coiling temperature. Simulated microstructures match those observed in a hot tandem mill and production of the hot-rolled coils with superior quality has been successfully achieved.

Keywords: Hot plane strain compression test, Isothermal annealing, Rolling temperature, Interpass time, Accumulated strain

1. INTRODUCTION

5052 aluminum alloy is used in a wide range of applications from beverage can ends, formable parts, to various 3C components having superior surface quality. Successful applications dictate a fully recrystallized microstructure under as hot-rolled condition. When fraction of recrystallized grains is low, defects of surface streaking or high earing ratio appear during the downstream processings.

To understand the evolution of microstructure during hot rolling, techniques have been explored. Pilot rolling linked with water quenching was widely used in Japan. Unless work rolls are well heated, large temperature drops occur and rolling temperature is hard to define. Quench time can be manually adjusted and be compatible to interpass time of a reverse mill because the time interval is relatively long. However, the interpass time is less than two seconds in a modern hot tandem mill so that this method can hardly be approached.

Hot-rolling simulators were thus developed and the experimental results were formulated as Eq.1,

$$t_{0.5}/\, d_{rex} = a \cdot d_o^{b} \cdot \varepsilon^{c} \cdot [\dot{\varepsilon} \cdot \exp(Q_{def}/R\,T_{def})]^{d} \cdot \exp(Q_{rex}/R\,T_{rex}) \quad \text{..... (1)}$$

where $t_{0.5}$, d_{rex}, d_o, ε, $\dot{\varepsilon}$, Q_{def}, R, T_{def}, Q_{rex} and T_{rex} denote time of 50% recrystallized, final grain size, initial grain size, strain, strain rate, activation for hot deformation, universal gas constant, deformation temperature, activation for annealing and annealing temperature and a, b, c, d are numerical constants, respectively. Compound factor $\dot{\varepsilon} \cdot \exp(Q_{def}/R\,T_{def})$ is Zener-Hollomon parameter.

On the basis of earlier reports, equations for aluminum alloys are listed in Table 1. Effect of rolling parameters, e.g., rolling temperature or strain, can be assessed accordingly. Nevertheless, mill application was found difficult because roles of accumulated strain, interpass time and coil cooling are undefined. The aim of this work was to identify their influences on the recrystallization behaviors of a 5052 aluminum alloy for the production of hot-rolled coils with superior quality.

2. EXPERIMENTAL

A transferred bar was cut as the starting material. Its chemical compositions are listed in Table 2 with the balanced composition of aluminum. Along the center part, samples of 25 mm (rolling direction) × 40 mm(b_o) × 12 mm (h_o) as shown Fig.1A were machined for plane strain compression test and they had an average grain size of 116± 10 μm (Fig.2).

Hot plane strain compression tests (Fig.1B) were carried out in a Gleeble 3800 simulator having a maximum force of 20 ton and strain rate, 120 s^{-1}. A typical heating cycle for a two-pass compression is demonstrated in Fig.3: samples were initially heated with 2°C/s to a predetermined temperature and soaked there for 30s, cooled with -5°C/s to the target temperature and soaked there for another 5s, then the first compression was made

Table 1 Published recrystallization equations for aluminum alloys[1-4]

Alloy	Prediction formula	Ref.
	Basic form: $t_{0.5}/ d_{rex}= a \cdot d_o^b \cdot \varepsilon^c \cdot [\dot{\varepsilon} \cdot \exp(Q_{def} /R\ T_{def})]^d \cdot \exp(Q_{rex} /R\ T_{rex})$	
5052	$t_{0.5}=1.25\times10^{-6} \cdot d_o^{1.35} \cdot \varepsilon^{-1.023} \cdot [\dot{\varepsilon} \cdot \exp(196{,}000/RT)]^{-0.66} \cdot \exp(200{,}000/RT)$	(1)
	$d_{rex}=8.463\times10^{3} \cdot \varepsilon^{-0.78} \cdot [\dot{\varepsilon} \cdot \exp(156{,}000/RT)]^{-0.113}$	
5182	$t_{0.5}=8.34\times10^{-7} \cdot d_o^{1.35} \cdot \varepsilon^{-0.93} \cdot [\dot{\varepsilon} \cdot \exp(196{,}000/RT)]^{-0.73} \cdot \exp(200{,}000/RT)$	(1)
	$d_{rex}=12.69\times10^{3} \cdot \varepsilon^{-0.37} \cdot [\dot{\varepsilon} \cdot \exp(156{,}000/RT)]^{-0.17}$	
5182	$t_{0.5}=[7.259\times10^{-7} \cdot [\dot{\varepsilon} \cdot \exp(187{,}800/RT)]^{-0.495} \cdot \exp(197{,}500/RT)]/ (4.879+ 2.81\cdot\varepsilon^2)$	(2)
	$d_{rex}=13.5\times d_o^{1.3} \cdot \varepsilon^{-0.5} \cdot [\dot{\varepsilon} \cdot \exp(187{,}800/RT)]^{-0.145}$	
Al-1Mg	$t_{0.5}=9.8\times10^{-6} \cdot d_o^{1.35} \cdot \varepsilon^{-2.7} \cdot [\dot{\varepsilon} \cdot \exp(156{,}000/RT)]^{-1.1} \cdot \exp(230{,}000/RT)$	(3)
	$d_{rex}=1.85\times10^{2} \cdot d_o^{1.3} \cdot \varepsilon^{-0.39} \cdot [\dot{\varepsilon} \cdot \exp(156{,}000/RT)]^{-0.24}$	
1×××	$t_{0.5}=1.5\times10^{-4} \cdot \varepsilon^{-1.5} \cdot [\dot{\varepsilon} \cdot \exp(158{,}000/RT)]^{-0.75} \cdot \exp(220{,}000/RT)$	(4)
	$d_{rex}=1.15\times10^{4} \cdot \varepsilon^{-0.5} \cdot [\dot{\varepsilon} \cdot \exp(158{,}000/RT)]^{-0.33} \cdot \exp(30{,}000/RT)$	

Table 2 Chemical compositions of the starting material (wt%).

Si	Fe	Cu	Mn	Mg	Cr
0.10	0.27	0.03	0.05	2.53	0.22

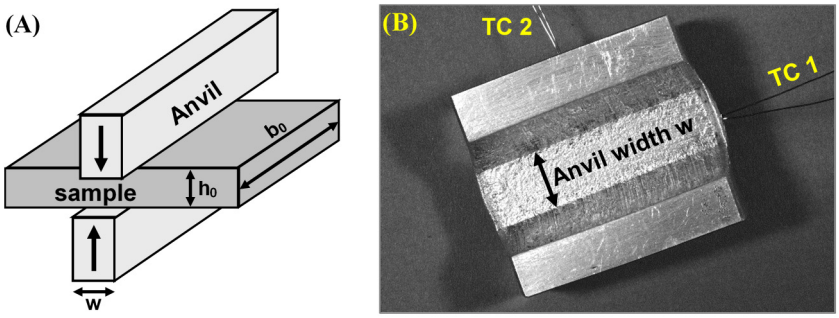

Fig.1. (A) Schematic diagram of plane strain compression test, (B) an as-compressed sample and thermal couples (TC 1and TC 2).

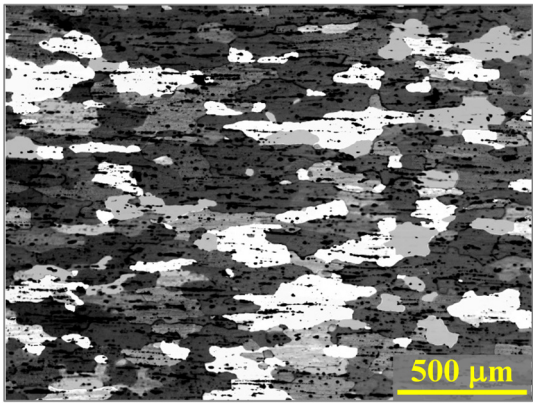

Fig.2. The starting material had an average grain size of 116 µm.

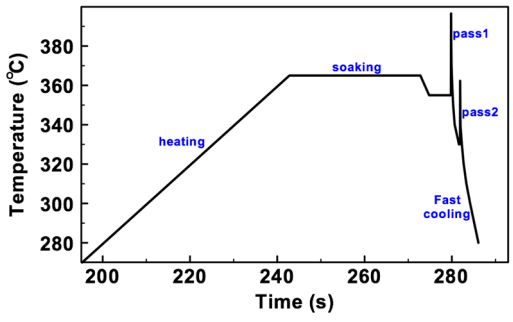

Fig.3. The heating cycle for a two-pass plane strain compression test.

where a sharp temperature rise can be seen. The second compression was subsequently made using a predetermined interpass time in a hot tandem mill. Immediately after the final compression, a cooling rate -60°C/s was introduced to preserve the deformed structure.

Fig.4 shows profiles of flow stress and sample temperature during a compression test. The stress increased sharply but displayed as wave forms during the initial 10ms because of load cell ringing. It was corrected using a moving averaged method as published elsewhere[5, 6]. A temperature rise of 40°C was observed. Since the compression was carried out with a constant strain rate, Zener-Hollomon parameter can be written as Eq.2 where T_i is instantaneous temperature and T_{def} can be derived by Eq.2a.

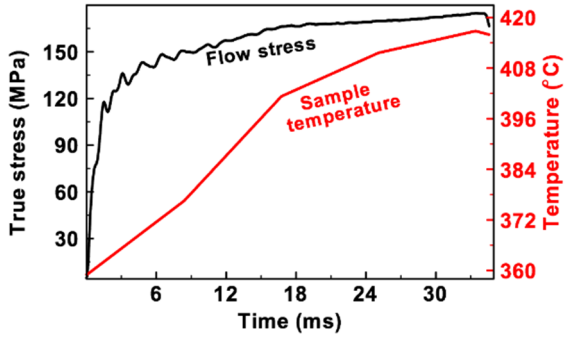

Fig.4. Profiles of flow stress and sample temperature during a compression test. (started at 360°C with strain 1.6 and strain rate 50 s^{-1})

$$Z = \dot{\varepsilon}\ [\exp(Q_{def}/RT_1) + \exp(Q_{def}/RT_2) + \ldots \exp(Q_{def}/RT_i)] = \dot{\varepsilon}\ \exp(Q_{def}/RT_{def}) \quad \ldots\ldots (2)$$

$$1/T_{def} = (1/i)\cdot \Sigma(1/T_1 + 1/T_2 + \ldots + 1/T_i) \quad \ldots\ldots (2a)$$

A programmable annealing furnace was used to simulate coil cooling of mill production. The furnace was heated to a sufficiently high temperature and cooled down at -80°C/h, similar to the cooling rate of a hot-rolled coil. When it dropped to the predetermined temperature, the as-compressed sample was put into the furnace and taken out for metallographic examination when cooled down to room temperature.

In addition, isothermal annealing was carried out for quantitative assessment over the parameter effects of hot rolling. Volume fraction of the recrystallized grains X_v was measured according to ASTM E562[7]. Observed data were fit into the Avrami equation (Eq.3) where t is annealing time, constants β and n were derived by a linear regression analysis. Accordingly, an isothermal recrystallization curve was constructed and Eq.3 was modified as Eq. 3a using the observed $t_{0.5}$ and n.

$$X_v = 1-\exp(-\beta t^n) \quad \ldots\ldots (3)$$

$$X_v = 1-\exp[-\mathrm{Ln}2\cdot (t_{rex}/t_{0.5})^n] \quad \ldots\ldots (3a)$$

When $t_{0.5}$ at other temperatures are available, Q_{rex} can be derived by the Arrhenius law (Eq. 4) where A is a constant and T is temperature, respectively[8].

$$1/t = A\cdot \exp(-Q_{rex}/RT) \quad \ldots\ldots (4)$$

Coil cooling was quantitatively assessed as follows. The cooling curve was transformed into tiny stepwise isothermal and isochronal segments as shown in Fig.5A. When coiling temperature T_1 drops to T_2 (Fig.5B), correction factor for t_2 is given in Eq.4a and that of t_i is similarly made for another temperature T_i. t_{rex}, overall effective anneal time at T_1 for the cooling curve, can be derived by Eq.4b through the aid of integration. X_v can be predicted when the t_{rex} is fit into Eq.3a.

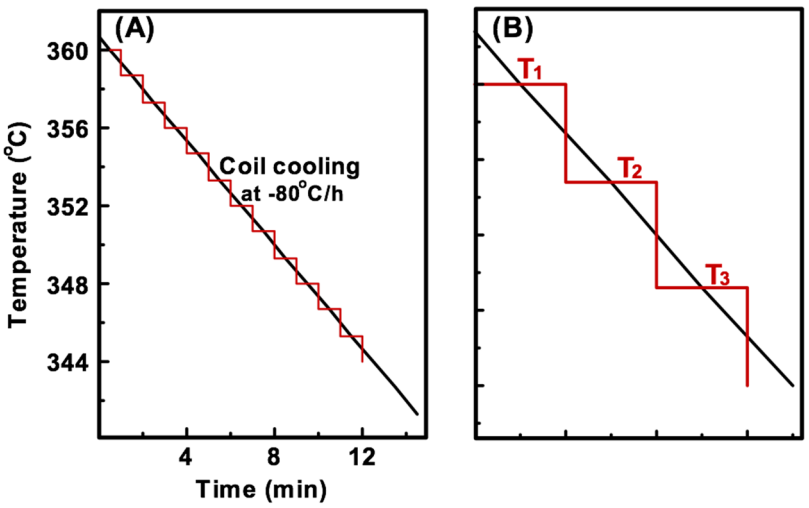

Fig.5. Coiling effect was assessed by (A) stepwise isothermal and isochronal function, (B) a close-up of A.

$t_2 = t_1 \cdot \exp[(Q_{rex}/R) \cdot (1/T_2 - 1/T_1)] \ldots$; $t_i = t_1 \cdot \exp[(Q_{rex}/R) \cdot (1/T_i - 1/T_1)]$ .....(4a)

$t_{rex} = \Sigma\, t_i = t_1 \cdot \exp\,[(Q_{rex}/R) \cdot (\Sigma 1/T_i - (i-1)/T_1)]$. (4b)

The nucleation rate N_a was measured from the early stage of recrystallization in each curve, e.g., when X_v was less than 30%. While d_{rex} was measured according to ASTM E112 from samples having X_v more than 95% [9]. Examinations with transmission electron microscopy (TEM) was carried out for the deformed samples.

3. RESULTS AND DISCUSSION

3.1 As-deformed microstructure

An as-deformed microstructure for the sample of Fig.4 is shown in Fig.6. It can be seen that in response to the vertical compression, the original grains (Fig.2) were flattened and greatly extended along the horizontal direction. No recrystallized grain was observed indicating that the fluctuations of flow stress (Fig.4) originated from load cell ringing rather than from the occurrence of dynamic recrystallization. Thus, it was confirmed that the cooling rate -60°C/s after the compression was fast enough to preserve the microstructure of hot-deformed samples.

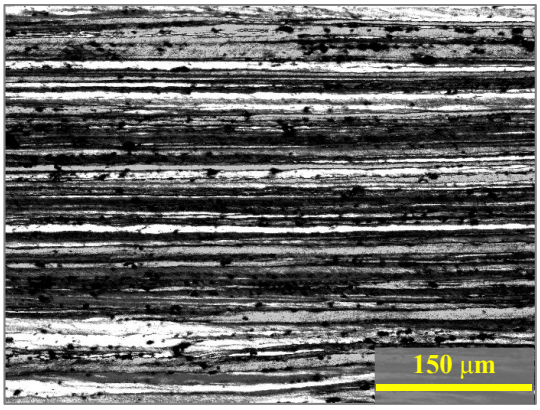

Fig.6. As-deformed microstructure for the sample of fig.4.

Examinations with TEM revealed that laminar structure in the deformed samples consisted of interlocked subgrains. Fig.7A shows a dark-field micrograph for the sample compressed at 300°C having an average size 0.5 μm. Subgrains coarsened to about 1.6 μm when the temperature was increased to 400°C (Fig.7B).

3.2 Simulated hot-rolled microstructure

The as-deformed sample of Fig.6 was subsequently annealed by a cooling cycle started from 360°C and cooled down at a rate of -80°C/h. Annealed grains (Fig.8) are similar to those of as-hot-rolled strips. Based on these results, it can be concluded that recrystallization occurs during the coiling stage of a hot rolling mill.

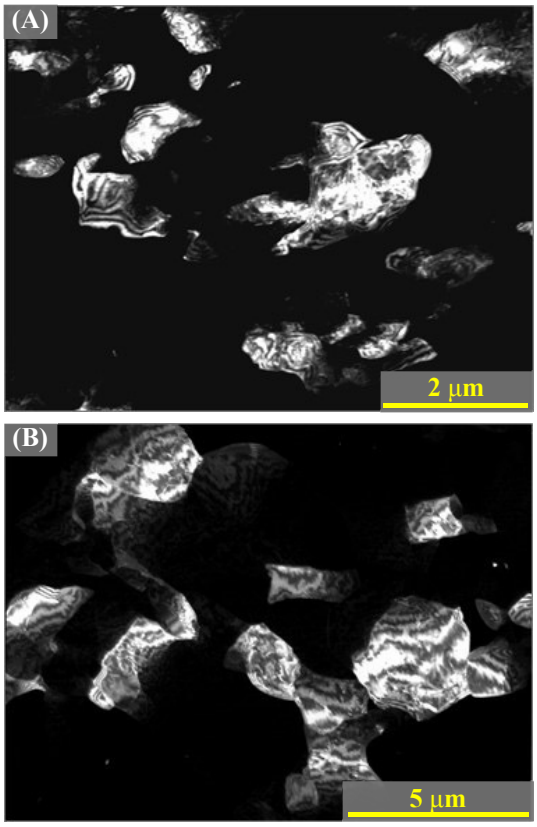

Fig.7. Dark-field image for a sample compressed at (A) 300°C and (B) 400°C having a strain of 1.6 and strain rate of 50 s^{-1}.

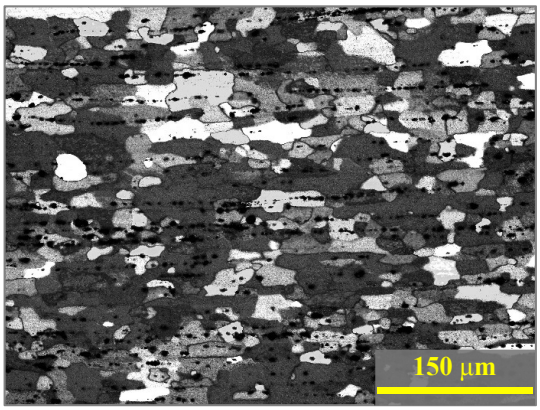

Fig.8. Microstructure of the as-deformed sample annealed by a cooling cycle to simulate mill coiling.

3.3 Parameter effect of single pass rolling

Effect of rolling temperature was assessed under the conditions of constant strain and strain rate. Fig.9 shows isothermal recrystallization curves over the start rolling temperatures from 300°C to 400°C. It is clear that the curve shifted to the left hand side with decreasing the temperature.

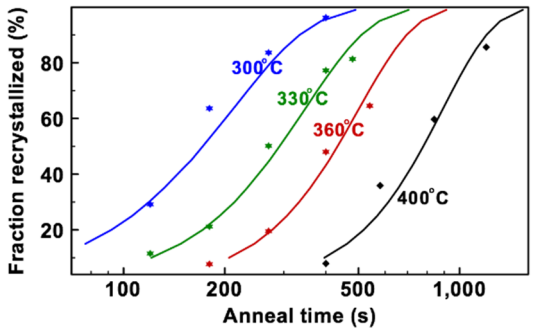

Fig.9. Isothermal recrystallization curves of samples having different rolling temperatures.

Results of recrystallization behaviors and flow stress are summarized in Table 3. Clearly, $t_{0.5}$ and d_{rex} increased with the temperature as predicted from the formula in Table 1. In contrast, N_a decreased with the temperature. While growth rate of the nucleated grains was found to fall within the range of 0.12- 0.20 μm/s regardless the temperature. It is considered that low nucleation rate resulted in coarse grains at high rolling temperatures. The observed $t_{0.5}$ was suitably fit by Eq.5. In addition, flow stress decreased with the temperature reflecting the coarsening effect of subgrain size as reported previously[10, 11].

$$\text{Ln } t_{0.5} = -6.5 \cdot 1000/T_{def} + 15.9 \quad \text{..... (5)}$$

Effect of strain rate was subsequently investigated during which challenges were encountered because of temperature variations as shown in Fig. 10. It can be seen that temperature rise occurred at higher strain rates while it dropped at $2s^{-1}$. T_{def} was kept at a relatively constant level by adjusting the start rolling temperatures. Parameter design and results of the strain rate effect are listed Table 4. It is clear that $t_{0.5}$ decreased, as formulated as Eq. 6; N_a and flow stress increased with the strain rate. Then effect of the strain rate was combined with that of rolling temperature as Zener-Hollomon parameter, another formulae Eq. 7 was obtained using the reported Q_{def} 200 KJ/mol[1]. It should be noted that linearity of the data based on Eq. 7 is governed by the value of Q_{def}.

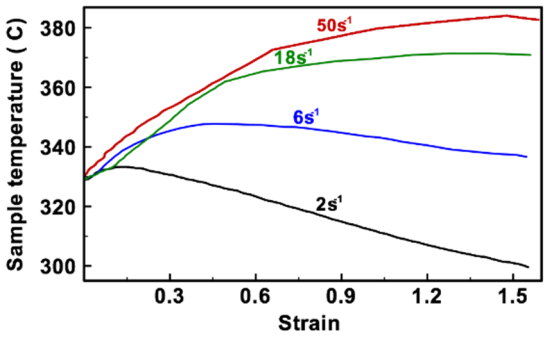

Fig.10. Temperature profiles during the compression for various strain rates.

$$\text{Ln } t_{0.5} = -0.14 \cdot \text{Ln } \cdot + 5.89 \quad \text{.....(6)}$$

$$\text{Ln } t_{0.5} = -0.25 \cdot \text{Ln } Z + 16.13 \quad \text{.....(7)}$$

Experiments over the effect of strain could be similarly made but in a hot tandem mill, several passes are consecutively rolled within a short time so that the applications of Table 3 and 4 are practically limited. For this, another approach using two-pass rolling was carried out.

Table 3 Effect of rolling temperature during single pass rolling.

T_{start}	T_{def}	$t_{0.5}$	d_{rex}	N_a	σ_{max}
300 °C	342 °C	175 s	30 μm	13.3/mm^2-s	210 MPa
330 °C	367 °C	291 s	30 μm	6.0/mm^2-s	190 MPa
360 °C	391 °C	433 s	37 μm	2.3/mm^2-s	176 MPa
400 °C	429 °C	738 s	51 μm	1.1/mm^2-s	162 MPa

Remarks: with common parameters of rolling strain 1.6, strain rate 50 s^{-1} and isothermal annealing at 340 °C. N_a denotes nucleation rate and μ_{max}, the maximum flow stress, respectively.

Table 4 Parameter design and the results of strain rate effect.

Strain rate	T_{start}	T_{def}	T_{peak}	$t_{0.5}$	N_a	σ_{max}
6 s^{-1}	330 °C	351 °C	356 °C	285 s	9.7/mm^2-s	165 MPa
18 s^{-1}	310 °C	350 °C	363 °C	242 s	8.3/mm^2-s	172 MPa
50 s^{-1}	308 °C	349 °C	379 °C	222 s	9.2/mm^2-s	177 MPa
120 s^{-1}	318 °C	349 °C	388 °C	183 s	14.3/mm^2-s	184 MPa

Remarks: isothermal annealing at 340 °C

3.4 Parameter effect of two-pass rolling

Parameter design of two-pass rolling is listed in Table 5 where strain rates and rolling temperatures were kept similarly, but the reduction in each case was adjusted as follows.

A: heavy reduction in pass 2.

B: equal reduction.

C: equal and light reduction.

D: longer t_{ip}, equal and light reduction.

E: longer t_{ip}, heavy reduction in pass 1.

F: single pass rolling.

Results of $t_{0.5}$, N_a and d_{rex} are summarized in the right columns of Table 5. It can be seen that $t_{0.5}$ and d_{rex} decreased with increasing the accumulated strain, arithmetic sum of the strains of pass 1 and 2. For instance, $t_{0.5}$ of samples A, B, E and F, the accumulated strain 1.6, were much shorter than those of samples C and D, the accumulated strain 1.4. Minor differences among the $t_{0.5}$ of samples A, B and E suggesting that recrystallization behavior remains similarly when heavy reduction in the pass 2 is moved forward to the pass 1. Thus, control of dimension quality becomes more efficient during mill production because flatness control is difficult when heavy reduction was made at the final pass.

Effect of interpass time can be found over the differences between samples C and D. It shows that $t_{0.5}$ increased with the interpass time presumably due to the recovery effect of the alloy. A short interpass time, i.e., high speed rolling, was reported to have merits by decreasing the earing ratio of the final products[12].

Quantitative formulation for the two-pass rolling suffered from the effect of the accumulated strain. For instance, sample D and E had the same reduction of final pass but different accumulated strain resulting in different recrystallization behaviors. Moreover, difficulties come from effects of rolling temperature (Table 3) and strain rate (Table 4). Although experimentally possible, it is impractical to mill application when both parameters for pass 1 and pass 2 are kept constantly. As a result, no further analysis over the parameter effect of two-pass rolling was made. On the other hand, annealing effect during coiling stage was quantitatively carried out.

Prior to this, Q_{rex} was measured using isothermal annealing curves for sample B as shown in Fig.11A. $t_{0.5}$ in the two curves are rearranged according to Arrhenius law as given in Fig.11B. The slope suggests an activation

Table 5 Parameters of two-pass rolling and experimental results.

Sample	Pass 1	t_{ip}	Pass 2	$t_{0.5}$	N_a	d_{rex}
A	380°C /40 s^{-1}/0.70	1.75 s	350°C /80 s^{-1}/0.90	161 s	13.1/mm^2-s	26 μm
B	370°C /40 s^{-1}/0.80	1.75 s	345°C /80 s^{-1}/0.80	154 s	12.4/mm^2-s	29 μm
C	370°C /40 s^{-1}/0.70	1.75 s	350°C /80 s^{-1}/0.70	195 s	5.7/mm^2-s	33 μm
D	370°C /40 s^{-1}/0.70	3.66 s	340°C /80 s^{-1}/0.70	265 s	2.4/mm^2-s	32 μm
E	380°C /40 s^{-1}/0.90	4.07 s	350°C /80 s^{-1}/0.70	190 s	8.4/mm^2-s	30 μm
F	-	-	340°C /50 s^{-1}/1.60	172 s	13.3/mm^2-s	30 μm

Remarks: t_{ip} denotes time interval between pass 1 and pass 2; isothermal annealing at 340 °C

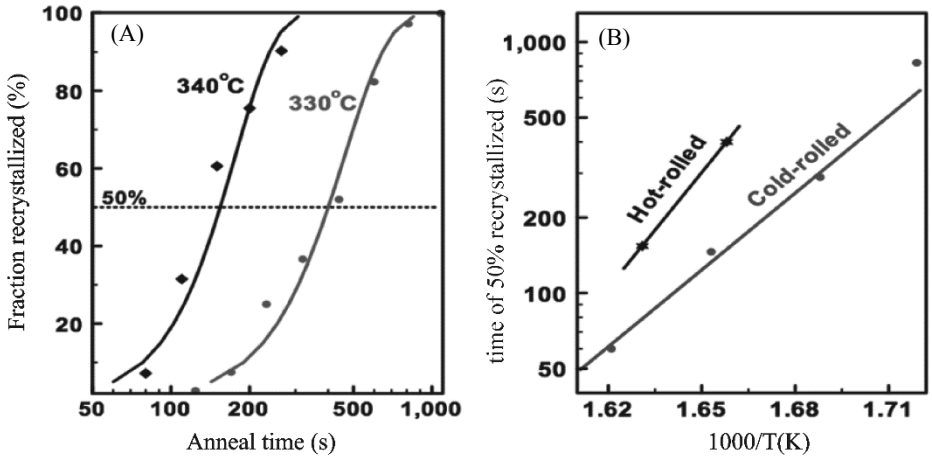

Fig.11. (A) Isothermal recrystallization curves for sample B, (B) measurements of activation energy for annealing.

energy for annealing 293 KJ/mol. It was slightly higher than that measured from the cold-rolled strips of the same starting material.

The observed Q_{rex} was fit into Eq. 4b for analyzing the annealing effect during the coiling process. Experimentally, the annealing furnace was heated to a high temperature and then cooled down at a rate -80°C/h. Samples were put into the furnace at 350°C, 338°C and 328°C, respectively.

Fig.12 shows a simulated microstructure annealed from 328°C. Experimental results are summarized in Table 6 where predicted t_{rex} were calculated according to Eq.4b using a reference temperature 340°C and X_v, by Eq.3b using the observed $t_{0.5}$ and n of isothermal annealing at the same temperature. Evidently, the predicted values are very close to the observed X_v as well as mill observations. Similar results were obtained when the cooling rate during coiling was changed. As a result, coiling temperature for the deformed sample could be predetermined to ensure a fully recrystallized condition.

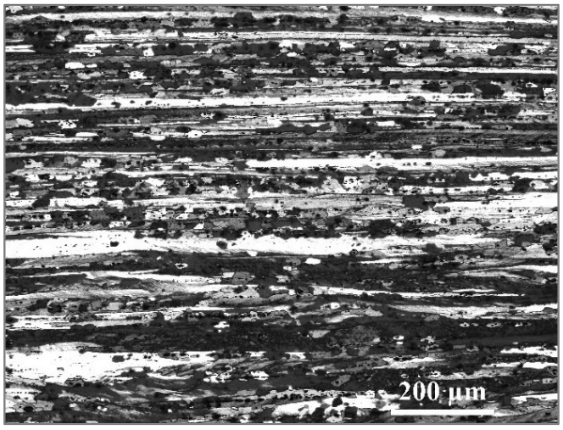

Fig.12. A simulated microstructure annealed from 328°C.

$$X_v = 1\text{-}\exp[-\mathrm{Ln}2\cdot (t_{rex}/200)^{2.28}] \quad \text{..... (3b)}$$

4. CONCLUSIONS

Evolution of microstructure in a 5052 hot-rolled strip has been thoroughly investigated by hot plane strain compression test with a Gleeble 3800 simulator. Hot-deformed samples were made using fast cooling at the end of the compression and annealed by a cooling curve of mill coiling to simulate the microstructure of hot-rolled strips. The curve was stepwised and quantitatively analyzed over the effect of coiling temperature and cooling rate. Isothermal annealings were also carried out to characterize the effect of rolling temperature, strain rate, accumulated strain and interpass time of a hot tandem mill. The following conclusions can be drawn on the basis of this present work.

1. A hot-deformed structure could be preserved by fast cooling at the end of the compression and it recrystallizes during the subsequent annealing.
2. Recrystallization of the deformed samples was promoted by decreasing rolling temperature, interpass time, or by increasing strain rate, accumulated strain as well as coiling temperature.
3. Activation for annealing was 293 KJ/mol for the hot-deformed samples being slightly higher than that of cold-rolled strips using the same material. It fit well with the observed annealing effect of coil cooling.

REFERENCES

1. M.A. Wells, D.J. Lloyd, I.V. Samarasekera, J. K. Brimacombe and E.B. Hawbolt: "Modeling the Microstructural Changes during Hot Tandem Rolling of AA5xxx Aluminum Alloys: part 1 Microstructural Evolution", Metall. Trans., 1998, 29B, pp. 611-620.
2. J. Hirsch, K. Karhausen, R. Kopp: Microstructure Simulation during Hot Rolling of Al-Mg Alloys, The 4th International Conference on Aluminum Alloys, 1994, pp.484-491.
3. Sellars, C.M., Irisarri, A.M., Puchi, E.S.: “Recrystallization Characteristics of Aluminium-1% Magnesium Under Hot Working Conditions”, in Microstructural Control in Aluminum Alloys: Deformation, Recovery and Recrystallization, E.H. Chia and H.J. McQueen, eds., Warrendale, Pennsylvania, The Metallurgical Society/AIME. 1986, pp. 179-186.
4. Gutierrez, I; Castro, F R; Urcola, J J; Fuentes, M.: “Static recrystallization kinetics of commercial purity aluminium after hot deformation within the steady state regime”. Mater. Sci. Eng., 1988, 102A.1,. pp. 77-84.

Table 6 Simulated results of coil cooling

Coiling temperature	350°C	338°C	328°C
Predicted t_{rex}	1060s	336s	125s
Predicted X_v	100%	90%	21%
Observed X_v	100%	88%	21%

Remarks: cooling rate was -80°C/h.

5. B. Roebuck, M. Brooks and M.G. Gee: Load Cell Ringing in High Rate Compression Tests, Applied Mechanics and Materials, 2004, vol. 1-2, pp. 205-210.
6. Shi-Rong Chen, Chung-Yung Wu, Yi-Liang Ou and Yen-Liang Yeh: "Hot Deformation Resistance of an AA5083 Alloy under High Strain Rate", 12th Asia-Pacific Conference on Engineering Plasticity and Its Appliaction, Key Engineering Materials 2015, Vol. 626 (2015) pp 553-560, (2015) Trans Tech Publications, Switzerland.
7. ASTM E562: "Standard Test Method for Determining Volume Fraction by Systematic Manual point count".
8. R.E. Reed-Hill: "Physical Metallurgy Principles", 2nd edition, 1973, pp.274.
9. ASTM E112- 2013: Standard Test Methods for Determining Average Grain Size.
10. Doko, T; Inabayashi, Y; Fujikura, C.: "Structural Variation During Hot Rolling at Lower Temperature of Aluminum Alloys", Journal of Japan Institute of Light Metals, 1991, vol. 41, 12, pp. 853-857.
11. T. Sheppard and M.A.Zaidi: "Influence of hot-working parameters on earing behavior of Al-2Mg sheet", Met. Tech., 1982, vol.9, pp. 368-374.
12. Suzuki, S., Matsumoto, H., Tajiri, A. and Muramatsu, T.: "Development of Aluminum Beverage Can Stocks", Furukawa-Sky Review, 2005, 1, pp. 3-8. □